

## Non-Fermi-liquid Kondo screening under Rabi driving

Seung-Sup B. Lee<sup>1</sup>, Jan von Delft<sup>1</sup>, and Moshe Goldstein<sup>2</sup>

<sup>1</sup>*Faculty of Physics, Arnold Sommerfeld Center for Theoretical Physics, Center for NanoScience, and Munich Center for Quantum Science and Technology, Ludwig-Maximilians-Universität München, Theresienstraße 37, 80333 München, Germany*

<sup>2</sup>*Raymond and Beverly Sackler School of Physics and Astronomy, Tel Aviv University, Tel Aviv 6997801, Israel*



(Received 5 June 2019; revised manuscript received 18 January 2020; accepted 27 January 2020; published 10 February 2020)

We investigate a Rabi-Kondo model describing an optically driven two-channel quantum dot device featuring a non-Fermi-liquid Kondo effect. Optically induced Rabi oscillation between the valence and conduction levels of the dot gives rise to a two-stage Kondo effect: Primary screening of the local spin is followed by secondary nonequilibrium screening of the local orbital degree of freedom. Using bosonization arguments and the numerical renormalization group, we compute the dot emission spectrum and residual entropy. Remarkably, both exhibit two-stage Kondo screening with non-Fermi-liquid properties at both stages.

DOI: [10.1103/PhysRevB.101.085110](https://doi.org/10.1103/PhysRevB.101.085110)

### I. INTRODUCTION

The Kondo effect, involving a local spin entangled with a bath of delocalized electrons, has been studied extensively in bulk systems and in transport through quantum dots. Some years ago, a landmark experiment [1] showed that it can also be probed optically: A weakly driven optical transition between the valence and conduction levels of the dot was used to abruptly switch the Kondo effect on or off, leaving telltale power-law signatures [2] in the dot emission spectrum. The case of strong spin-selective optical driving was subsequently studied theoretically within the context of a single-channel Rabi-Kondo (1CRK) model [3], involving Rabi oscillations between the dot valence and conduction levels. This was predicted to lead to nonequilibrium quantum-correlated state featuring two-stage Kondo screening: The local spin is screened by a primary screening cloud via the single-channel Kondo (1CK) effect, then the Rabi-driven levels by a larger, secondary screening cloud. Despite its nonequilibrium nature, this state has a simple Fermi-liquid (FL) description in terms of scattering phase shifts, since only a single screening channel is involved.

This raises an intriguing question: What type of nonequilibrium state will arise when the Rabi-driven dot couples to *two* spinful channels, described by a two-channel Rabi-Kondo (2CRK) model? Without Rabi driving, it reduces to the standard two-channel Kondo (2CK) model, known to have a non-Fermi liquid (NFL) ground state [4], describable by Bethe Ansatz [5–7], conformal field theory (CFT) [8–10] or bosonization [11–14]. However, NFL physics is known to be very sensitive to perturbations such as channel asymmetry or a magnetic field. Do the NFL properties survive under Rabi driving? If so, what are their fingerprints? In this paper, we answer these questions. We use a combination of bosonization arguments and numerical renormalization group (NRG) [15–17] calculations to compute the 2CRK emission spectrum and impurity entropy. We find that NFL behavior survives, and, remarkably, leaves clear fingerprints in the emission in both the primary *and* secondary screening regimes.

The rest of this paper is organized as follows. In Sec. II, we introduce our system, the 2CRK model. In Sec. III, we provide a qualitative description of the screening processes in the 2CRK model. In Secs. IV and V, we study the impurity contribution to the entropy and the Kondo cloud, respectively. In Sec. VI, the main points of our bosonization approach are outlined. In Sec. VII, we analyze the emission spectrum. We conclude in Sec. VIII. The Appendix offers the details of our bosonization approach.

### II. TWO-CHANNEL RABI-KONDO MODEL

In this section, we first introduce the system in the laboratory frame and then derive the effective Hamiltonian in the rotating frame to be treated by NRG and bosonization.

We consider a small quantum dot ( $d$ ) with a conduction ( $c$ ) and a valence ( $v$ ) level as the impurity, and two large dots as the bath [Fig. 1(a)]. The small dot is modeled by the Hamiltonian

$$H_d = \sum_{x=c,v} \left[ \frac{U_{xx}}{2} n_x (n_x - 1) + \epsilon_x n_x \right] + U_{cv} n_c n_v, \quad (1)$$

where  $n_x = \sum_{\sigma} d_{x\sigma}^{\dagger} d_{x\sigma}$  denotes the particle number operator for the  $x$  level ( $x = c, v$ ), and  $d_{x\sigma}$  annihilates spin- $\sigma$  electron at the  $x$  level of energy  $\epsilon_x$ .  $U_{cc}$ ,  $U_{vv}$ , and  $U_{cv}$  are the Coulomb interaction strengths. The level separation  $\epsilon_c - \epsilon_v$  is of the order of the semiconductor band gap  $\sim 1$  eV. We consider the parameter regime in which the ground states of the small dot have  $(n_c, n_v) = (1, 2)$  in the absence of the Rabi driving to be introduced next.

We introduce a laser applied to the small dot, which induces Rabi oscillation between the  $c$  and  $v$  levels. A circularly polarized laser would have coupled to one spin species due to an optical selection rule [3, 18]. In the following, we will consider the case of linearly polarized light, which symmetrically couples to both spin states. The laser frequency  $\omega_L$  is chosen to be close to the bare dot transition between  $(n_c, n_v) = (1, 2)$  states and  $(n_c, n_v) = (2, 1)$  states, i.e.,

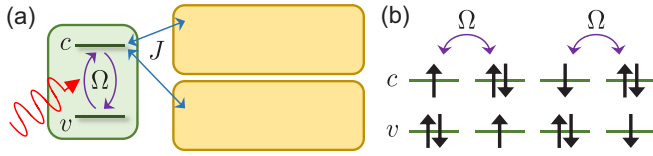


FIG. 1. (a) Schematic depiction of the 2CRK model in the laboratory frame. A small dot with two levels (conduction  $c$  and valence  $v$ ) has its  $c$  level coupled to two large dots via spin exchange  $J$ . The analogous 1CRK model has only one large dot. Linearly polarized laser induces Rabi oscillation of frequency  $\Omega$  in which electrons transition between the  $c$  and  $v$  levels, accompanied by the absorption and emission of light. (b) The states of the small dot having  $n_d = n_c + n_v = 3$  electrons. The states of  $(n_c, n_v) = (2, 1)$  are connected to the states of  $(n_c, n_v) = (1, 2)$  via the Rabi oscillation. In the rotating frame, the  $c$ - $v$  coupling becomes time independent with amplitude  $\Omega$ .

$\omega_L \simeq U_{cc} + \epsilon_c - U_{vv} - \epsilon_v$ . (We set  $\hbar = k_B = 1$ .) Hence the  $(n_c, n_v) = (2, 1)$  states are accessed via the Rabi oscillation from the  $(n_c, n_v) = (1, 2)$  states [see Fig. 1(b)]. The other states of  $n_d = n_c + n_v \neq 3$  can be accessed only via virtual processes due to the energy cost of the Coulomb interaction.

Since the optical transition is close to the material's band gap, that is, of order 1 eV, and much larger than all the other energy scales (which are typically not more than a few tens of meV), one could make the rotating wave approximation, under which a transfer of electron from the  $v$  to the  $c$  level involves the absorption of a photon and vice versa. We will further assume that the laser can be described as a classical field, and hence that spontaneous emission could be neglected. Then the light-induced Hamiltonian term in the laboratory frame is given by

$$H_L^{(\text{lab})} = \Omega \sum_{\sigma} (d_{c\sigma}^{\dagger} d_{v\sigma} e^{-i\omega_L t} + \text{H.c.}), \quad (2)$$

where  $\Omega$  is the Rabi frequency.

In addition, the  $c$  level of the small dot is symmetrically tunnel-coupled to two identical large dots (channels  $\ell = 1, 2$ ). These are assumed large enough to have essentially continuous excitation spectra, yet small enough that their charging energies suppress interchannel charge transfer. That is,  $n_d + N_1$  and  $n_d + N_2$  do not fluctuate, where  $N_{\ell}$  means the particle number at the large dot  $\ell$ . Under these conditions, the whole system Hamiltonian in the laboratory frame can be approximated via the Schrieffer-Wolff transformation [19] and up to an overall constant, by

$$H^{(\text{lab})} = \sum_{\ell} J \vec{S}_c \cdot \vec{s}_{\ell} + \delta_L n_v + H_{\text{bath}} + \Omega \sum_{\sigma} (d_{c\sigma}^{\dagger} d_{v\sigma} e^{-i\omega_L t} + \text{H.c.}), \quad (3)$$

where the Hilbert space for the small dot is restricted to the four-dimensional subspace of  $n_d = 3$  shown in Fig. 1(b). Here  $\vec{S}_c = \sum_{\sigma\sigma'} d_{c\sigma}^{\dagger} \frac{1}{2} \vec{\sigma}_{\sigma\sigma'} d_{c\sigma'}$  and  $\vec{s}_{\ell} = \sum_{\sigma\sigma'} \int_{-D}^D d\epsilon d\epsilon' \frac{1}{2D} c_{\ell\sigma}^{\dagger} \frac{1}{2} \vec{\sigma}_{\sigma\sigma'} c_{\ell\sigma'}$  are  $c$ -level and  $\ell$ -channel spin operators, respectively.  $H_{\text{bath}} = \sum_{\ell\sigma} \int_{-D}^D d\epsilon \in c_{\ell\sigma}^{\dagger} c_{\ell\sigma}$  describes the large dots with half-bandwidth  $D$ , and  $c_{\ell\sigma}$  annihilates channel- $\ell$  electron of energy  $\epsilon$  and

spin  $\sigma$ . The coupling strength  $J$  is proportional to  $1/(U_{cc} + 2U_{cv} + \epsilon_c) - 1/(2U_{cv} + \epsilon_c)$ .

We will now go to the rotating frame with respect to the laser-mode Hamiltonian, via the transformation  $\mathcal{U} = e^{i\omega_L n_v t}$ . The rotating-frame Hamiltonian  $H^{(\text{rot})} = \mathcal{U}^{\dagger} H^{(\text{lab})} \mathcal{U} + i(d\mathcal{U}^{\dagger}/dt)\mathcal{U}$  will become time independent,

$$H^{(\text{rot})} = \sum_{\ell} J \vec{S}_c \cdot \vec{s}_{\ell} + \delta_L n_v + H_{\text{bath}} + \Omega \sum_{\sigma} (d_{c\sigma}^{\dagger} d_{v\sigma} + \text{H.c.}), \quad (4)$$

where  $\delta_L = \omega_L - (U_{cc} + \epsilon_c - U_{vv} - \epsilon_v)$  is the detuning of the laser frequency from the bare dot transition. This is the 2CRK Hamiltonian to be studied in the rest of this paper. For reference, we also include some results for the analogous 1CRK model ( $\ell = 1$  only) and the standard 2CK and 1CK models (without  $v$  level).

Since the coupling to the fermionic bath is assumed to be the main relaxation mechanism and dominates over spontaneous emission, the system would relax to an electronic equilibrium state in the rotating frame, which corresponds to a time-dependent state in the laboratory frame. Thus we can analyze the system in the rotating frame, employing equilibrium concepts such as entropy.

Note that our setup, which is driven optically, is different from previous setups driven by ac magnetic field [20,21] in two key aspects. First, the laser can be focused within the length scale of optical wavelength, so one can selectively drive the small dot only. This selectivity has been demonstrated in experiments [1]. Second, the rotating wave approximation works very well for our system, since the energy scale of the laser frequency is larger than the other energy scales in the system by at least two orders of magnitude. The selectivity and the rotating wave approximation are, however, unlikely for the systems driven by ac magnetic field that are in the microwave or rf regime.

### III. QUALITATIVE CONSIDERATIONS

Without Rabi driving,  $\Omega = 0$ , the ‘‘trion’’ and ‘‘Kondo’’ sectors, with  $c$  and  $v$  level occupancies  $(n_c, n_v) = (2, 1)$  and  $(1, 2)$ , respectively, are decoupled, and the  $v$  level is inert. The trion sector is a trivial FL, with the doubly occupied  $c$  level forming a local spin singlet. The Kondo sector constitutes a standard Kondo model, involving the spin of the singly occupied  $c$  level. Below a characteristic Kondo temperature  $T_K$ , it will be screened by bath electrons. For the 2CRK model, it is overscreened, leading to NFL behavior characteristic of the 2CK model. For the 1CRK model, it is fully screened, showing standard 1CK FL behavior.

For *weak driving*,  $0 < \Omega \ll T_K$ , Rabi oscillations between the  $c$  and  $v$  levels couple the Kondo and trion sectors. Then primary screening of the  $c$ -level spin, occurring at energies  $\lesssim T_K$ , will be followed by secondary screening of  $c$ - $v$  transitions at the renormalized Rabi coupling  $\Omega^*$  (as in Ref. [3]), provided that the ground-state energies of the two (decoupled) sectors differ by less than  $\Omega^*$ . (A precise definition of  $\Omega^*$  will be given later.) We thus fine-tune  $\delta_L$  such that for  $\Omega = 0$  the Kondo and trion ground states are degenerate, following a strategy discussed in the Supplemental Fig. S2 of Ref. [3].

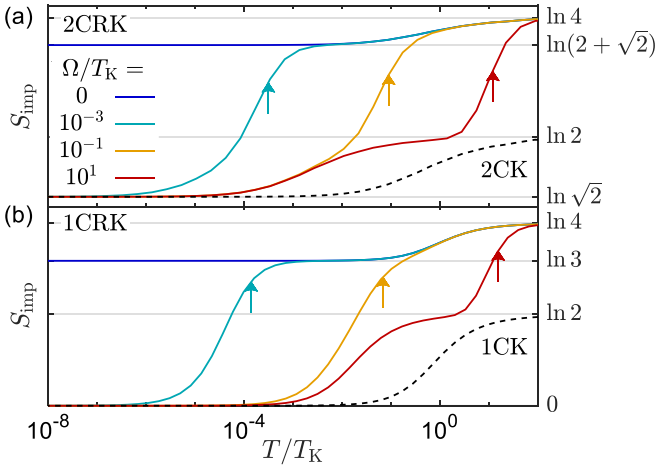


FIG. 2. Impurity contribution to the entropy,  $S_{\text{imp}}$ , for the (a) 2CRK and (b) 1CRK models, for four  $\Omega$ -values (solid lines). Arrows indicate the corresponding values of  $\omega_{\text{max}}/T_K$ , the energy scale associated with the peak in the emission spectrum shown in Fig. 4. For comparison, dashed lines show  $S_{\text{imp}}$  for the standard 2CK and 1CK models, respectively, for the same value of  $J$ .

Finally, for *strong driving*,  $\Omega \gtrsim T_K$ , the Rabi coupling generates a strong splitting of bonding and antibonding states built from the  $c$  and  $v$  levels. The local spin of the bonding state will then undergo single-stage screening, as for the standard 2CK or 1CK models.

These qualitative arguments will be substantiated quantitatively below by NRG calculations and bosonization arguments. For the former, we use  $J = 0.28D$  throughout, leading to  $T_K^{2\text{CRK}} \simeq 3 \times 10^{-4}D$  and  $T_K^{1\text{CRK}} \simeq 4 \times 10^{-4}D$  when  $\Omega = 0$ . The bath discretization grid is set by  $\Lambda^{2\text{CRK}} = 4$  and  $\Lambda^{1\text{CRK}} = 2.7$ , and no  $z$  averaging is used. We use the QSpace tensor library [22] to exploit the SU(2) symmetries of spin and channel where applicable.

#### IV. ENTROPY

Figures 2(a) and 2(b) show our NRG results for the impurity contribution to the entropy [16],  $S_{\text{imp}}$ , which quantifies the effective degrees of freedom of the dot at different temperatures. At high temperatures,  $T \gg T_K$ ,  $\Omega$ , the entropy  $S_{\text{imp}} = \ln 4$  simply counts all four configurations of the dot [Fig. 2(b)] for both the 2CRK and 1CRK models. At lower temperatures, the behavior of the entropy depends on the relation of  $\Omega$  and  $T_K$ .

For strong driving  $\Omega \gtrsim T_K$ , only two bonding states with different spins are accessible for  $T < \Omega$ . Hence  $S_{\text{imp}}(T \lesssim \Omega)$  shows a plateau at  $\ln(2)$ , followed by a single crossover to  $T = 0$  value of  $\frac{1}{2} \ln(2) = \ln(\sqrt{2})$  or  $\ln(1) = 0$  for the 2CRK or 1CRK models, respectively. These values are the same as in the standard 2CK or 1CK models [6–8] (shown as dashed lines), respectively. They reflect overscreening of a local spin by two spinful channels (resulting in a decoupled local Majorana mode [11–14]), or its complete screening by a single spinful channel [23] (resulting in a spin singlet), respectively.

In contrast, for weak driving  $0 < \Omega \ll T_K$ , two-stage screening occurs. For intermediate temperatures,

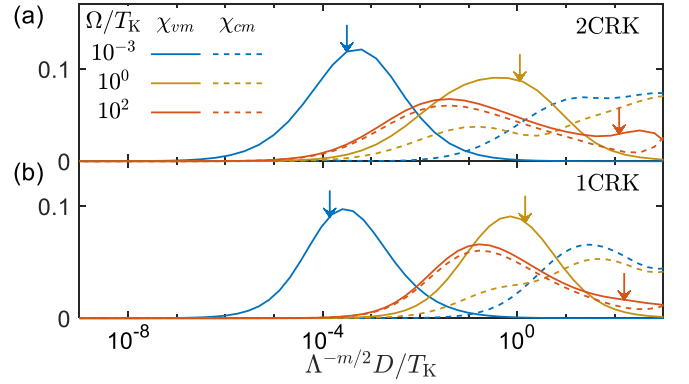


FIG. 3. Spin-spin correlators between the impurity and bath spin operators, revealing the structure of the screening clouds for the (a) 2CRK and (b) 1CRK models. We display  $\chi_{vm} = -4\langle P_{\uparrow} S_{vz} S_{mz} \rangle / \langle P_{\uparrow} \rangle$  (solid) and  $\chi_{cm} = -4\langle P_{\uparrow} S_{cz} S_{mz} \rangle / \langle P_{\uparrow} \rangle$  (dashed), where  $S_{vz}$ ,  $S_{cz}$ , and  $S_{mz}$  are  $z$ -component spin operators for the  $v$  level,  $c$  level, and the Wilson chain site  $m \geq 0$ , respectively. Site  $m = 0$  is directly coupled to the  $c$  level.  $P_{\uparrow} = \sum_{\sigma} n_{v\sigma} (1 - n_{v\bar{\sigma}}) n_{c\uparrow} n_{c\downarrow}$  and  $P_{\uparrow} = \sum_{\sigma} n_{v\uparrow} n_{v\downarrow} n_{c\sigma} (1 - n_{c\bar{\sigma}})$  are projectors onto the trion and Kondo sectors, involving a singly occupied  $v$  or  $c$  level, respectively. Both  $\chi_{vm}$  and  $\chi_{cm}$  are obtained by averaging two lines, interpolating odd and even  $m$ 's, respectively. We choose the abscissa as  $\Lambda^{-m/2} D/T_K$ , where  $\Lambda^{-m/2} D$  is the energy scale (and also the inverse length scale [15,24]) associated with the chain site  $m$ . For strong driving (red),  $\chi_{cm}$  and  $\chi_{vm}$  have coinciding peaks, reflecting single-stage screening of the bonding-level spin. In contrast, for intermediate (yellow) and weak (blue) driving, we observe two-stage screening: the peaks of  $\chi_{cm}$ , reflecting the screening of the  $c$ -level spin, occur at higher energies than those of  $\chi_{vm}$ , reflecting the screening of the  $c$ - $v$  transitions. The area under each peak is  $\simeq 1$ . Arrows indicate the corresponding values of  $\omega_{\text{max}}/T_K$ .

$S_{\text{imp}}(\Omega^* \ll T \ll T_K)$  shows a primary-screening plateau at  $\ln(2 + \sqrt{2})$  or  $\ln(2 + 1)$  for the 2CRK or 1CRK models: the NFL- or FL-screened local spin contributes  $\sqrt{2}$  or 1 to the local degeneracy count, with another 2 from the two trion ( $v$ ) states. At the lowest temperatures,  $T \ll \Omega^*$ , the  $c$ - $v$  transitions lead to a secondary-screening limiting value of  $S_{\text{imp}} = \ln \sqrt{2}$  or 0 for the 2CRK and 1CRK models, respectively, as for the standard 2CK and 1CK models. Finally, for  $\Omega = 0$  (i.e.,  $\omega_{\text{max}} = 0$ ), the primary-screening plateau in  $S_{\text{imp}}$  persists down to  $T = 0$ .

#### V. KONDO CLOUDS

To further study the nature of the screening clouds involved in primary and secondary screening, we have computed spin-spin correlation functions between the impurity and bath spin operators, see Fig. 3. As described in the caption thereof, for weak driving we find a nested, two-stage cloud, screening the  $c$ -level spin at energies  $\gtrsim T_K$ , and  $c$ - $v$  transitions at energies  $\simeq \omega_{\text{max}}$ . In contrast, for strong driving we find just a single screening cloud.

#### VI. BOSONIZATION

We proceed to a more detailed analysis of the weak driving case,  $0 < \Omega \ll T_K$ , using bosonization (since the methods

of Ref. [3] do not easily generalize to the 2CRK model). Here we outline the main points, relegating further details to the Appendix. With uniaxial anisotropy, the bosonized form [11–14] of the 2CRK Hamiltonian  $H_{\text{bath}} + H_d$  is

$$H = \sum_{\ell=1,2} \left\{ \frac{u}{4\pi} \int_{-\infty}^{\infty} dx [\partial_x \phi_{\ell}(x)]^2 + \frac{J_z}{\pi\sqrt{2}} P_K S_z \partial_x \phi_{\ell}(0) + \frac{J_{xy}}{2\pi a} P_K (S_{\pm} e^{i\sqrt{2}\phi_{\ell}(0)} + \text{H.c.}) \right\} + 2\Omega\tau_x, \quad (5)$$

where  $S_{\pm} = S_x \pm iS_y$ , while  $\tau_{\pm} = \sum_{\sigma} d_{c\sigma}^{\dagger} d_{v\sigma}$ ,  $\tau_{-} = \tau_{\pm}^{\dagger}$ , and  $\tau_z = n_c - n_v$  are Pauli matrices in the orbital  $c$ - $v$  (Kondo-trion) pseudospin space, and  $P_K = (1 + \tau_z)/2$  is a projector onto the Kondo sector. In addition,  $u$  and  $a = D/u$  are the Fermi velocity and lattice spacing (inverse momentum cutoff), and  $\phi_{\ell}(x)$  is the chiral (unfolded) bosonic spin field (the charge sector decouples). It obeys the commutation relation  $[\phi_{\ell}(x), \phi_{\ell}(x')] = i\pi \text{sgn}(x - x')$ , where  $\partial_x \phi_{\ell}(0)/(\pi\sqrt{2})$  is the density of the  $z$  component of the channel- $\ell$  electron spin density at the dot site.

### A. 1CRK

Let us start from the single-channel case, where  $\ell = 1$  [ $\phi_2(x)$  does not exist]. The unitary transformation  $U_{\alpha} = e^{-i\alpha S_z P_K \phi_1(0)}$  with  $\alpha = J_z/(\pi\sqrt{2}u)$  eliminates the  $J_z$  term at the cost of modifying the  $J_{xy}$  term by a shift to the coefficient of  $\phi_1(0)$  in the exponent.

At energies  $\gg T_K \gg \Omega$ , we may ignore the Rabi term, and follow the usual perturbative renormalization group (RG) flow of the 1CK problem.  $J_{xy}$  flows since it has a nontrivial scaling dimension, set by the corresponding bosonic exponent (after the above-mentioned transformation). In addition, second-order spin-flip ( $J_{xy}$ ) processes revive the non-spin-flip  $J_z$  term, which may then be transformed away as above.  $J_z$  thus flows to a fixed-point value,  $J_z = 2\pi u$ , corresponding to the Kondo fixed-point  $\pi/2$  phase shift, while  $J_{xy}$  grows until it becomes of the order of the reduced cutoff, which could serve to define the primary  $c$ -spin Kondo scale  $T_K$ . The  $U_{\alpha}$ -type transformations applied throughout the RG flow modify the Rabi term. Thus, below  $T_K$  we obtain the following intermediate-scale effective Hamiltonian:

$$H_{\text{1CRK}}^{\text{int}} = \frac{u}{4\pi} \int_{-\infty}^{\infty} dx [\partial_x \phi_1(x)]^2 + \frac{J_{xy}^{\text{ren}}}{\pi a} P_K S_x + \Omega\tau_{\pm} [P_{\uparrow} e^{-i\phi_1(0)/\sqrt{2}} + P_{\downarrow} e^{i\phi_1(0)/\sqrt{2}}] + \text{H.c.}, \quad (6)$$

where  $P_{\uparrow,\downarrow} = 1/2 \pm S_z$  is a projector into the subspace  $S_z = \pm 1/2$  and  $J_{xy}^{\text{ren}} \sim T_K \gg \Omega$ . The latter large coupling fixes the dot spin to  $S_x = 1/2$ , which corresponds, in the original basis, to an entangled state of the impurity and bath spins, i.e., the primary Kondo singlet. Thus  $P_{\uparrow,\downarrow}$  are replaced by their expectation values  $\langle P_{\uparrow,\downarrow} \rangle = 1/2$ . The resulting model describes the hybridization between the pseudospin ( $c$ - $v$  or Kondo-trion) degree of freedom and the channel, which is equivalent (up to a transformation similar to  $U_{\alpha}$  but involving  $\tau_z$  instead of  $S_z$ ) to an anisotropic Kondo model for the pseudospin space. The Rabi coupling  $\Omega$  is relevant, with scaling dimension  $\eta_1 = 1/4$ , determined by the corresponding bosonic exponent in Eq. (6), or, within CFT, from its role as boundary condition

changing operator, turning on and off 1CK screening [25]. Hence,  $\Omega$  flows to strong coupling, creating a new scale, the renormalized Rabi frequency (secondary Kondo temperature),  $\Omega^* \sim T_K(\Omega/T_K)^{1/(1-\eta_1)} = T_K(\Omega/T_K)^{4/3} \ll \Omega$ , where one expects a peak in the dot emission spectrum to occur, instead of the more usual peak at  $\Omega$  for strong driving  $\Omega \gg T_K$ . Below this scale, the pseudospin is screened by the creation of a secondary ‘‘Kondo singlet.’’

### B. 2CRK

Let us now perform a similar analysis of the 2CRK model. Defining the fields  $\phi_{\pm}(x) = [\phi_1(x) \pm \phi_2(x)]/\sqrt{2}$ , only the former couples to  $J_z$ , and could be eliminated by a transformation similar to  $U_{\alpha}$  defined with  $\sqrt{2}\phi_{\pm}(0)$  instead of  $\phi_1(0)$ . For  $\Omega \ll T_K$ , one may proceed with the primary 2CK RG flow, which drives  $J_z$  to  $\pi u$ , corresponding to a  $\pi/4$  phase shift, and  $J_{xy}$  to  $J_{xy}^{\text{ren}} \propto T_K \gg \Omega$ . At the same time, the Rabi coupling gets modified. On the scale of  $T_K$ , we thus arrive at

$$H_{\text{2CRK}}^{\text{int}} = \sum_{p=\pm} \frac{u}{4\pi} \int_{-\infty}^{\infty} dx [\partial_x \phi_p(x)]^2 + \frac{J_{xy}^{\text{ren}}}{\pi a} P_K S_x \cos \phi_{-}(0) + \Omega\tau_{\pm} [P_{\uparrow} e^{-i\phi_{+}(0)/2} + P_{\downarrow} e^{i\phi_{+}(0)/2}] + \text{H.c.} \quad (7)$$

The first line describes the 2CK fixed point, at which the  $\phi_{-}$  remains coupled:  $S_x$  assumes a definite value  $S_x = \pm 1/2$  and, correspondingly,  $\phi_{-}(0)$  is locked to a minimum or maximum of the cosine function. Refermionizing the local spin- $\phi_{-}$  system, the  $J_{xy}$  term couples a local Majorana fermion ( $\propto S_x$ ) to the lead, leaving another local Majorana ( $\propto S_y$ ) unscreened [11,12].

We now turn to the second line. Since  $J_{xy}^{\text{ren}} \sim T_K \gg \Omega$ , we may again set  $P_{\uparrow,\downarrow} \rightarrow 1/2$ . The remaining term is a product of  $\tau_{\pm}$  with bosonic exponents. The exponents contribute  $1/8$  to the scaling dimension of  $\Omega$ , while  $\tau_{\pm}$  turns on or off the  $J_{xy}^{\text{ren}}$  term, which is equivalent to turning on or off a local backscattering impurity in a Luttinger liquid, with scaling dimension  $1/16$  [26,27]. Thus, the overall scaling dimension of  $\Omega$  is  $\eta_2 = 3/16$ . This matches the corresponding CFT analysis of its role as a boundary-condition changing operator [25]. Thus,  $\Omega$  is relevant, flowing to strong coupling and generating a new scale  $\Omega^* \sim T_K(\Omega/T_K)^{1/(1-\eta_2)} = T_K(\Omega/T_K)^{16/13} \ll \Omega$ , below which secondary screening of the  $c$ - $v$  (Kondo-trion) fluctuations is achieved. Importantly, since the Rabi term is spin symmetric, it does not interfere with the primary NFL 2CK screening, and leaves the decoupled Majorana ( $S_y$ ) unscreened: While the Rabi term contains  $S_z \propto S_x S_y$ , the corresponding processes are suppressed by the dominant  $J_{xy}^{\text{ren}}$  term, and all higher order (in  $\Omega$ ) processes which leave the system within the low-energy manifold of  $J_{xy}^{\text{ren}}$  term do not couple to  $S_y$ .

## VII. EMISSION SPECTRUM

Having established the general picture of the two-stage NFL screening, we can now analyze its effect on the main experimental observable, the dot emission spectrum. The emission spectrum of linear polarization at detuning  $\omega$  from the driving laser frequency is proportional to the spectral

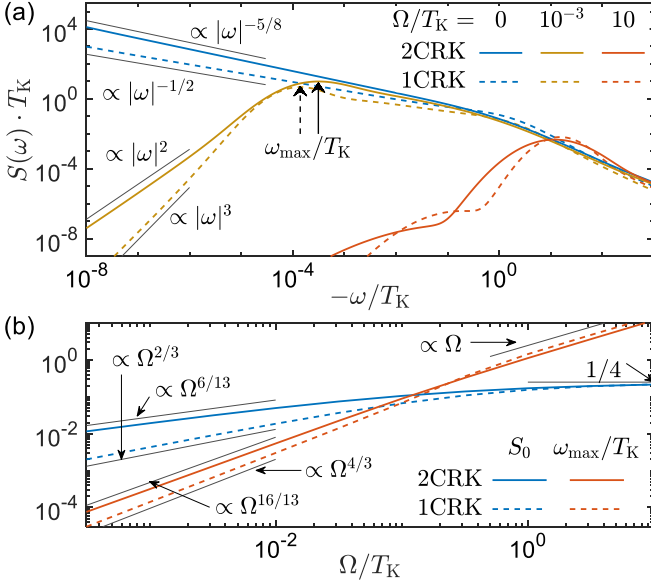


FIG. 4. (a) Log-log plot of the emission spectrum  $S(\omega)$ , and (b) its finite-frequency peak position  $\omega_{\max}$  and zero-frequency spectral weight  $S_0$  as functions of Rabi driving  $\Omega/T_K$ , for the 2CRK (solid) and 1CRK (dashed) models at  $T = 0$ . Guide-to-the-eye grey lines depict the power laws predicted by bosonization arguments (see text).

function [3],

$$S(\omega) = \sum_{jj'} \rho_j |\langle j' | \sum_{\sigma} d_{v\sigma}^{\dagger} d_{c\sigma} | j \rangle|^2 \delta(\omega + E_j - E_{j'}), \quad (8)$$

where  $|j\rangle$  and  $E_j$  are energy eigenstates and eigenvalues of the Rabi-Kondo Hamiltonian, and  $\rho_j = e^{-E_j/T}/Z$ . This is the spectral function of the Rabi term with itself. At temperature  $T = 0$ , the emission spectrum has weight only for  $\omega \leq 0$ . Without Rabi driving,  $S(\omega \rightarrow 0^-)$  shows a power-law divergence. For weak driving, the divergence is cut off, giving way to a power-law decrease. Accordingly, a wide peak at  $|\omega| = \omega_{\max}$  and a delta-function peak  $S_0 \delta(\omega)$  of weight  $S_0$  at  $\omega = 0$  emerge. We identify  $\omega_{\max}$  with the renormalized Rabi frequency  $\Omega^*$ .

Figure 4(a) shows a log-log plot of the emission spectrum, revealing its various power laws. For weak driving, there are two distinct regimes: (i) The intermediate-detuning regime,  $\omega_{\max} \lesssim |\omega| \lesssim T_K$ , is dominated by the Kondo exchange coupling and reflects primary screening. Here the correlations of the Rabi term with itself are governed by its scaling dimension  $\eta$ , giving  $S(\omega) \propto |\omega|^{2\eta-1}$  with  $\eta = \eta_1 = 1/4$  and  $\eta = \eta_2 = 3/16$  for the 1CRK or 2CRK models, respectively. Thus, this part of the spectrum reveals the scaling of 1CK versus 2CK boundary condition changing operators [25]. (ii) The small-detuning regime,  $|\omega| \lesssim \omega_{\max}$ , is dominated by the Rabi coupling and reflects secondary  $c$ - $v$  screening. In this regime,  $S(\omega)$  corresponds to the correlation function of the exchange interaction  $\sum_{\ell} \vec{S} \cdot \vec{s}_{\ell}$  with itself in the standard Kondo models, which yields  $S(\omega) \propto |\omega|^3$  and  $\propto |\omega|^2$  for the 1CRK and 2CRK models, respectively. The power is reduced in the 2CRK case, as the unscreened Majorana  $S_y$  appearing in the Rabi term in Eq. (7) (through  $S_z \propto S_x S_y$ ) reduces the corresponding

scaling dimension by  $1/2$ . Thus, the  $|\omega|^2$  behavior is a clear fingerprint of the NFL nature of the nonequilibrium secondary screening nature in the 2CRK system.

Figure 4(b) shows that  $\omega_{\max}$  and  $S_0$  increase as power laws in  $\Omega$ . For weak driving, our previous analysis shows that, in accordance with the numerical data,  $\omega_{\max} \sim \Omega^* \propto \Omega^{1/(1-\eta)} \sim \Omega^{16/13}$  or  $\Omega^{4/3}$ , and moreover (as we will momentarily explain),  $S_0 \sim \Omega^{2\eta/(1-\eta)} \sim \Omega^{6/13}$  or  $\Omega^{2/3}$  for the 2CRK or 1CRK models, respectively. Indeed,  $S_0$  takes up the spectral weight missing at small detuning due to  $\Omega^*$  cutting off the intermediate detuning  $S(\omega) \propto |\omega|^{2\eta-1}$  behavior. Hence,  $S_0 \propto \int_0^{\Omega^*} d\omega |\omega|^{2\eta-1} \sim \Omega^{2\eta/(1-\eta)}$ . Alternatively, by Eq. (8),  $S_0$  is the square of the expectation value of  $\tau_x$  (before transformations) in the ground state. But  $\tau_x$  is the Rabi term divided by  $\Omega$  and the Rabi term should scale as  $\Omega^*$ , leading to  $S_0 \sim (\Omega^*/\Omega)^2 \sim \Omega^{2\eta/(1-\eta)}$ , as before. Thus, the Kondo boundary condition changing operators governs both  $\omega_{\max}$  and  $S_0$ . For strong driving,  $\omega_{\max} \sim \Omega$  corresponds to the transition energy between the bonding and antibonding states of  $c$  and  $v$  levels.

## VIII. CONCLUSIONS

We have identified a two-stage NFL screening process in a Rabi driven quantum dot. The NFL nature survives in nonequilibrium as the Rabi driving respects both spin and channel symmetries. We have developed a new bosonization approach that explains the power-law exponents obtained numerically. The distinct power laws in the emission spectra should motivate optical spectroscopy studies on the multichannel quantum dot devices. The case of non-negligible spontaneous emission, which goes beyond the description of the time-independent Hamiltonian in the rotating frame, would be an interesting question for future study. We envision our findings to also be relevant for higher-dimensional driven strongly correlated materials.

## ACKNOWLEDGMENTS

We thank E. Sela for useful discussions. This joint work was supported by German Israeli Foundation (Grant No. I-1259-303.10). S.-S.B.L. and J.v.D. are supported by the Deutsche Forschungsgemeinschaft (DFG, German Research Foundation) under Germany's Excellence Strategy – EXC-2111 – 390814868; S.-S.B.L. further by Grant No. LE 3883/2-1. M.G. acknowledges support by the Israel Science Foundation (Grant No. 227/15), the US-Israel Binational Science Foundation (Grant No. 2016224), and the Israel Ministry of Science and Technology (Contract No. 3-12419).

## APPENDIX: BOSONIZATION DETAILS

In this Appendix, we develop in detail the theory of the multichannel Kondo effect by first reviewing the bosonization description of the ordinary single- and two-channel Kondo (1CK, 2CK), then going on to their Rabi-Kondo versions, without and with spin rotation symmetry (the latter being the case considered in the main text).

We note that the Yuval-Anderson (YA) Coulomb gas approach [28–33] is known to give equivalent results to the bosonization approach for all universal (i.e., cutoff-independent) quantities, such as critical dimensions.

Meanwhile, the Coulomb gas approach provides more accurate microscopic expressions for the phase shifts that are cutoff dependent. We have verified that the same is true for the systems discussed in this paper. However, in this paper, we employ the bosonization approach, since it is more succinct than the Coulomb gas approach.

### 1. Ordinary Kondo

First, we review the ordinary (equilibrium) 1CK and 2CK effects from the bosonization perspective.

#### a. Single-channel ordinary Kondo

Let us start from the ordinary single-channel Kondo effect. Using a bosonic description of the channel, the charge sector decouples, while the spin sector can be written in terms of a single right-moving chiral boson over the entire 1D line (instead of a single nonchiral boson on the 1D half-line), leading to the following Hamiltonian [11,34]:

$$H_{1\text{CK}} = \frac{u}{4\pi} \int_{-\infty}^{\infty} dx [\partial_x \phi(x)]^2 + \frac{J_z}{\pi\sqrt{2}} S_z \partial_x \phi(0) + \frac{J_{xy}}{2\pi a} (S_+ e^{i\sqrt{2}\phi(0)} + \text{H.c.}), \quad (\text{A1})$$

where  $S_{\pm} = S_x \pm iS_y$ ,  $S_{x,y,z}$  are the impurity spin-1/2 operators,  $u$  and  $a$  are the Fermi velocity and lattice spacing (inverse momentum cutoff), the bosonic field obeys the commutation relation  $[\phi(x), \phi(x')] = i\pi \text{sgn}(x - x')$ , and  $\partial_x \phi(0)/(\pi\sqrt{2})$  is the conduction electron spin density at the dot site. Applying the transformation  $H_{1\text{CK}} \rightarrow H'_{1\text{CK}} = U_{\alpha} H_{1\text{CK}} U_{\alpha}^{\dagger}$  where  $U_{\alpha} = e^{-i\alpha S_z \phi(0)}$  with  $\alpha = J_z/(\pi\sqrt{2}u)$ , the  $J_z$  term is eliminated, at the cost of modifying the exponent in the  $J_{xy}$  term:

$$H'_{1\text{CK}} = \frac{u}{4\pi} \int_{-\infty}^{\infty} dx [\partial_x \phi(x)]^2 + \frac{J_{xy}}{2\pi a} (S_+ e^{i\sqrt{2}[1-J_z/(2\pi v)]\phi(0)} + \text{H.c.}), \quad (\text{A2})$$

We now proceed with perturbative RG, using Cardy's operator product expansion (OPE) version [35].  $J_{xy}$  flows because it has a nontrivial scaling dimension (due to the corresponding nontrivial bosonic exponent), whereas the OPE of the two  $J_{xy}$  terms reintroduces the  $J_z$  term. This can be transformed again into the bosonic exponent. Defining the dimensionless exchange couplings  $\mathcal{J}_{xy,z} = J_{xy,z}/(2\pi u)$  and denoting the energy cutoff by  $D = v/a$ , we thus obtain Anderson's well-known RG equations:

$$-D \frac{d\mathcal{J}_{xy}}{dD} = [1 - (1 - \mathcal{J}_z)^2] \mathcal{J}_{xy}, \quad (\text{A3})$$

$$-D \frac{d\mathcal{J}_z}{dD} = (1 - \mathcal{J}_z) \mathcal{J}_{xy}^2. \quad (\text{A4})$$

Thus,  $\mathcal{J}_z$  flows to the strong-coupling fixed point value  $\mathcal{J}_z = 1$  ( $\pi/2$  phase shift). At that point, the impurity spin becomes decoupled from the bath—the exchange term becomes simply  $\propto \mathcal{J}_{xy} S_x$  (where at strong coupling  $\mathcal{J}_{xy} \propto T_K$ , the Kondo temperature), and seemingly polarized the impurity spin in the  $x$  direction. Recalling that the  $S_x$  operator has undergone a succession of transformations dressing it with the bosonic field, we recognize that, in terms of the original

fields, this actually signifies (an anisotropic version of) the Kondo singlet. Indeed, the fact that the spin flip terms in the original Hamiltonian,  $S_{\pm} e^{\pm i\sqrt{2}\phi(0)}$ , have been renormalized to  $S_{\pm}$  means that the renormalized versions of the original  $S_{\pm}$  operators are  $S_{\pm} e^{\mp i\sqrt{2}\phi(0)}$ . The correlation function of these two operators decays in time as  $1/t^2$  (due to the bosonic factor), in accordance with FL theory (in which one posits that at the fixed point the impurity spin “merges” with the Fermi sea, so its correlator behaves like the correlation function of the lead fermion density). Another way to get this result is to notice that, generically (that is, in a higher order RG than what we considered),  $S_z$  could get dressed by the lead spin density at the impurity site,  $\propto \partial_x \phi(0)$ , hence its correlation would decay as  $1/t^2$ . Using similar arguments, the connected correlation function of the exchange terms in the original Hamiltonian turns into a connected correlator of two lead spin operators with two lead spin operators, decaying as  $1/t^4$ , translating into an  $\omega^3$  behavior of the corresponding spectral function at low frequencies. Finally, since the impurity Hamiltonian reduces to  $\propto \mathcal{J}_{xy} S_x$  at the fixed point, if a magnetic field in the  $z$  direction is introduced, the impurity susceptibility becomes  $\propto \mathcal{J}_{xy}^{-1} \propto T_K^{-1}$ . This will also give a finite expectation value to the lead spin correlators, making the leading contribution (at long time) to the exchange-exchange correlation function decay as  $1/t^2$ , or  $\omega$  in the frequency domain. Finally, the impurity entropy is  $\ln 2$  at  $T \gg T_K$ , and goes to zero at  $T \ll T_K$ , due to the Kondo screening.

#### b. Two-channel ordinary Kondo

Now the starting Hamiltonian is

$$H_{2\text{CK}} = \sum_{\ell=1,2} \left\{ \frac{u}{4\pi} \int_{-\infty}^{\infty} dx [\partial_x \phi_{\ell}(x)]^2 + \frac{J_z}{\pi\sqrt{2}} S_z \partial_x \phi_{\ell}(0) + \frac{J_{xy}}{2\pi a} S_+ e^{i\sqrt{2}\phi_{\ell}(0)} + \text{H.c.} \right\}, \quad (\text{A5})$$

where  $\ell = 1, 2$  labels the two conduction electron channels,  $\partial_x \phi_{\ell}(0)/(\pi\sqrt{2})$  gives their respective spin densities at the dot site, and we assume channel symmetry. Here it is useful to define the symmetric and antisymmetric combinations,  $\phi_{\pm}(x) = [\phi_L(x) \pm \phi_R(x)]/\sqrt{2}$ , which keep the commutation relations the same. We now apply the transformation  $U_{\alpha\pm} = e^{-i\alpha S_z \phi_{\pm}(0)}$  with  $\alpha = J_z/(\pi u)$  to eliminate the  $J_z$  term and get

$$H_{2\text{CK}} = \sum_{p=\pm} \frac{u}{4\pi} \int_{-\infty}^{\infty} dx [\partial_x \phi_p(x)]^2 + \frac{J_{xy}}{\pi a} S_+ \cos[\phi_{-}(0)] (e^{i[1-J_z/(\pi v)]\phi_{+}(0)} + \text{H.c.}). \quad (\text{A6})$$

The RG equations are similar to the 1CK case, but with  $(1 - \mathcal{J}_z) \rightarrow (1 - 2\mathcal{J}_z)$ . Hence,  $\mathcal{J}_z$  flows to a value of  $1/2$  ( $\pi/4$  phase shift), at which point the impurity remains coupled only to  $\phi_{-}$ .  $J_{xy}$  continues to flow to strong coupling, where it becomes  $\propto T_K$  (this strong coupling bosonic description corresponds to the intermediate coupling NFL fixed point in the traditional description in terms of the original fermions). If one re-fermionizes the local spin and the bosonic subsystem  $\phi_{-}$ , the  $J_{xy}$  term becomes a coupling of a local Majorana operator ( $S_x$ ) to a Majorana field density in the lead at the

adjacent site, namely,  $\cos[\phi_-(0)]$ , while  $S_y$  becomes a local decoupled Majorana. This is the famous Emery-Kivelson point. Therefore, the low-temperature impurity entropy is  $\ln \sqrt{2}$ . Since  $S_z \propto iS_x S_y$ , its correlator with itself is a convolution of the correlators of a localized Majorana fermion ( $\propto S_y$ ) and a propagating one ( $\propto S_x$ ), and decays in time as  $1/t$ , as that of one free fermion times one localized fermion, leading to a logarithmic divergence of the susceptibility with the largest cutoff energy (magnetic field, temperature, or frequency). For a similar reason, the original non-spin-flip exchange term,  $\propto S_z \partial_x \phi_+(0)$ , has correlations decaying as  $1/t^3$ , implying a low-frequency power-law behavior of  $\omega^2$ , in the absence of a magnetic field (a magnetic field suppresses the NFL 2CK physics and restores the FL 1CK  $\omega$  behavior). If we look at correlators of  $S_+$  (with its conjugate), we can use the fact that the series of transformations map it to  $S_+ e^{-i\phi_+(0)}$ , leading to a  $1/t$  behavior, similar to  $S_z$ .

One can recover the behavior of the susceptibility using purely bosonic language [36–39]. At the strong  $J_{xy}$  fixed point,  $S_x$  picks a value  $\pm 1/2$  and then  $\phi_-(0)$  is pinned to either a minimum or a maximum of the cosine function, respectively. With that, one can calculate the susceptibility, that is, the retarded correlator of  $S_z$  with itself. Indeed,  $S_z$  anticommutes with  $S_x$ , hence with the spin-flip exchange term. Since the spin-flip exchange term modifies by unity the spin of one of the leads, the operator  $V = e^{i\pi N_-}$ , where  $N_- = N_1 - N_2$  is the difference between the refermionized populations of the two leads (corresponding to  $S_z$  of the original electrons, since the bosonic fields are all related to the original electronic spin degrees of freedom), also anticommutes with the spin-flip exchange term. Hence, the correlator of  $S_z$  could be replaced by a correlator of  $V$ . Conservation of the overall refermionized population,  $N_+ = N_1 - N_2$  allows one to write replace  $V \rightarrow e^{i2\pi N_1} = e^{i\phi_1(0)}$ . Remembering that at the fixed point the two leads are effectively well coupled,  $N_1$  behaves as the population of one half of an infinite lead. With this, the correlation function of  $V$  with itself decays in time as  $1/t$ , again leading to a logarithmic divergence of the susceptibility with the largest cutoff energy (magnetic field, temperature, or frequency).

## 2. Spin-asymmetric Rabi-Kondo

We now add to the Kondo effect a laser, which tries to Rabi flip the electron constituting the impurity spin into a level decoupled from the leads. We will introduce a corresponding two-level degree of freedom, with Pauli matrices  $\tau_{x,y,z}$ , whose two states  $\tau_z = \pm 1$  correspond to the electron in the coupled conduction ( $c$ ) level (Kondo) and in the valence ( $v$ ) level (trion), respectively. The Rabi flopping ( $\tau_x$ ) is induced by a laser with amplitude  $\Omega$ . If the laser has a proper circular polarization, it only couples to a spin-up electron,  $S_z = 1/2$ .

### a. Single-channel spin-asymmetric Rabi-Kondo

Let us start from the single-channel spin-asymmetric Rabi-Kondo (1CARK) case, analyzed in our previous work [3]. Based on all the above considerations, the Hamiltonian is

$$H_{\text{1CARK}} = \frac{u}{4\pi} \int_{-\infty}^{\infty} dx [\partial_x \phi(x)]^2 + \frac{J_z}{\pi\sqrt{2}} P_K S_z \partial_x \phi(0) + \frac{J_{xy}}{2\pi a} P_K (S_+ e^{i\sqrt{2}\phi(0)} + \text{H.c.}) + 2\Omega \tau_x P_\uparrow. \quad (\text{A7})$$

Here  $P_K = \frac{1}{2}(1 + \tau_z)$  acts as a local projector onto the  $c$  level (i.e., the Kondo sector) and  $P_\uparrow = \frac{1}{2} + S_z$  as a local projector onto the spin-up subspace. We will concentrate on the case where the Kondo temperature is much larger than the Rabi frequency,  $T_K \gg \Omega$ . Then, at energy scales larger than  $T_K$ , we can ignore the Rabi term. The transformations and RG flow are as above, with the only difference that every transformation  $U_\alpha = e^{-i\alpha S_z \phi(0)}$  should be replaced by  $U_\alpha = e^{-i\alpha(1+\tau_z)S_z \phi(0)/2}$ . The series of transformations on the way to the Kondo fixed point at  $\mathcal{J}_z = 1$  then modifies the Rabi term, giving

$$H_{\text{1CARK}}^{\text{int}} = \frac{u}{4\pi} \int_{-\infty}^{\infty} dx [\partial_x \phi(x)]^2 + \frac{J_{xy}^{\text{ren}}}{\pi a} P_K S_x + \Omega P_\uparrow (\tau_+ e^{-i\phi(0)/\sqrt{2}} + \text{H.c.}), \quad (\text{A8})$$

where  $J_{xy}^{\text{ren}} \propto T_K (\gg \Omega)$ , as mentioned above. Thus, the corresponding Kondo term is much larger than the Rabi term and effectively eliminates the  $S_z$  part of  $P_\uparrow = \frac{1}{2} + S_z$  (the eliminated part breaks the symmetry under  $S_z \rightarrow -S_z$  on the scale  $\Omega^*$  introduced below, as a local magnetic field would do, but this has a negligible effect in the current 1CK physics, since  $\Omega^* \ll T_K$ ). With this, the Rabi term looks exactly like the spin-flip exchange term in the pure Kondo problem, Eq. (A2), demonstrating that the Rabi term leads to a secondary Kondo screening process. The scaling dimension, say  $\eta_1$ , of the 1CRK term is dictated by the bosonic exponent, giving  $\eta_1 = 1/4$ , reflecting the Anderson orthogonality catastrophe with a phase shift change of  $\pi/2$  in each spin channel caused by a Rabi flop. It can also be thought of as a boundary condition changing operator (from Kondo to non-Kondo), and CFT analysis [25] gives the same result for its scaling dimension. As a result, for frequencies in the range  $\Omega^* \ll |\omega| \ll T_K$  (where the new low-energy scale  $\Omega^*$  will be defined shortly), the emission spectrum (imaginary part of the retarded correlator of the Rabi term with itself) scales as  $|\omega|^{2\eta_1-1} = |\omega|^{-1/2}$ . Moreover, the RG equation for  $\Omega$  is [35]

$$-D \frac{d(\Omega/D)}{dD} = (1 - \eta_1) \frac{\Omega}{D}, \quad (\text{A9})$$

with solution  $\Omega(D)/D = \Omega/T_K (D/T_K)^{\eta_1-1}$ , where we have taken into account that the RG flow of  $\Omega$  starts at the scale of  $T_K$ . Therefore,  $\Omega(D)$  flows to strong coupling. The scale at which  $\Omega(D)/D$  becomes of order unity defines the renormalized Rabi frequency (secondary Kondo temperature),  $\Omega^*/T_K \sim (\Omega/T_K)^{1/(1-\eta_1)} = (\Omega/T_K)^{4/3}$ . Thus, the impurity entropy starts with the value  $\ln 3$  at  $T \gg T_K$  (the four possible values of  $S_z$  and  $\tau_z$ , except the excluded possibility of  $\tau_z = -1$  and  $S_z = -1/2$ ), then decreases to  $\ln 2$  for  $\Omega^* \ll T \ll T_K$  (due to the Kondo screening of the  $\tau_z = 1$  sector), and then goes to zero for  $T \ll \Omega^*$ , due to the secondary Kondo screening.

Below  $\Omega^*$ , secondary Kondo screening (of the  $\tau$  degree of freedom) sets in. The emission spectrum, which corresponds to a correlator of the Rabi term with itself, becomes the spectral function of the correlator of the secondary Kondo exchange term with itself. Our previous analysis for the single-channel case shows that this leads to an  $|\omega|^3$  behavior, or, in the presence of detuning (which adds to the Hamiltonian a term proportional to  $\tau_z$ , that is, a magnetic field in the

secondary Kondo language), to an  $|\omega|$  scaling. Also, at zero frequency a delta function appears in the emission spectrum. Its amplitude can be calculated in two ways. One is to note that the spectral weight missing by the emergence of  $\Omega$  and the corresponding change of the spectral function from  $\propto |\omega|^{2\eta_1-1}$  to a positive power should go into the delta function, giving it a weight scaling as  $\int_0^{\Omega^*} d\omega |\omega|^{2\eta_1-1} \sim \Omega^{*2\eta_1} \sim \Omega^{2\eta_1/(1-\eta_1)} = \Omega^{2/3}$ . The other argument is that the coefficient of the delta function is  $|\langle G|\tau_x|G\rangle|^2$ , the square of the matrix element of  $\tau_x$  (before the transformations) between the ground state and itself, and this matrix element is the ground-state expectation value of the Rabi term divided by  $\Omega$ . The expectation value of the Rabi term scales as  $\Omega^*$ , giving again an  $(\Omega^*/\Omega)^2 = \Omega^{2\eta_1/(1-\eta_1)} = \Omega^{2/3}$  scaling of the weight of the delta function.

### b. Two-channel spin-asymmetric Rabi-Kondo

We will now consider the analogous two-channel spin-asymmetric Rabi-Kondo (2CARK) setup. Now the starting Hamiltonian is

$$H_{2\text{CARK}} = \sum_{\ell=1,2} \left\{ \frac{u}{4\pi} \int_{-\infty}^{\infty} dx [\partial_x \phi_{\ell}(x)]^2 + \frac{J_z}{\pi\sqrt{2}} P_K S_z \partial_x \phi_{\ell}(0) + \frac{J_{xy}}{2\pi a} P_K (S_+ e^{i\sqrt{2}\phi_{\ell}(0)} + \text{H.c.}) \right\} + 2\Omega P_{\uparrow} \tau_x. \quad (\text{A10})$$

At energies larger than  $T_K$ , we can use similar steps to the above and arrive at

$$H_{2\text{CARK}}^{\text{int}} = \sum_{p=\pm} \frac{u}{4\pi} \int_{-\infty}^{\infty} dx [\partial_x \phi_{\ell}(x)]^2 + \frac{J_{xy}^{\text{ren}}}{\pi a} P_K S_x \cos[\phi_{-}(0)] + \Omega P_{\uparrow} (\tau_+ e^{-i\phi_{+}(0)/2} + \text{H.c.}). \quad (\text{A11})$$

For the 2CRK model, the scaling dimension, say  $\eta_2$ , of the Rabi term, seen as a boundary condition changing operator, is given by  $\eta_2 = 3/16$  [25]. One could arrive at this value using also our abelian bosonization language: The  $\phi_+$  exponent contributes 1/8 to the scaling dimension of the Rabi term. Beyond that, the  $\tau_{\pm}$  operators turn on or off the transformed Kondo exchange term involving  $\cos[\phi_{-}(0)]$ . Now, turning on and off such a cosine appears in the problem of the Fermi edge singularity, that is, turning on and off backscattering by impurity in a Luttinger liquid. This problem was analyzed in Refs. [26,27]. They showed that, at long times, the cosine can be replaced by a quadratic term (since it is relevant), which allows one to find its contribution to the long time behavior of the correlation function of  $\tau_x$ . This contribution scales as  $t^{-1/8}$ , corresponding to a scaling dimension of 1/16. Adding this to the 1/8 contributed by the exponential of  $\phi_+$ , we recover the CFT result  $\eta_2 = 3/16$ . Thus, for  $\Omega^* \ll |\omega| \ll T_K$  the emission spectrum behaves as  $|\omega|^{2\eta_2-1} = |\omega|^{-5/8}$ . The RG equation for  $\Omega$  is the same as above, with  $\eta_2$  taking the place of  $\eta_1$ , reflecting the different scaling dimension of the Rabi term. Then we get a low-energy scale  $\Omega^* \propto \Omega^{1/(1-\eta_2)} = \Omega^{16/13}$ , and the weight of the delta peak at zero frequency scales as  $(\Omega^*)^{2\eta_2} \propto \Omega^{2\eta_2/(1-\eta_2)} = \Omega^{6/13}$ . The impurity entropy will be  $\ln 3$  for  $T \gg T_K$ ,  $\ln(1 + \sqrt{2})$  (2CK partial screening + exciton state) for  $\Omega^* \ll T \ll T_K$  and zero for  $T \ll T_K$ .

As for the behavior of the emission spectrum at  $|\omega| \ll \Omega^*$ , one could argue that the Rabi term, with its explicit  $S_z$  dependence, breaks the symmetry for flipping  $S_z$  and has similar effects to a local magnetic field on the physical spin. Thus, below  $\Omega^*$  the 2CK physics should be suppressed, and one should recover the 1CK behavior of  $|\omega|^3$  or  $|\omega|$  in the absence or presence of detuning, respectively.

### 3. Spin-symmetric Rabi-Kondo

Finally, we arrive at the spin-symmetric version of the Rabi-Kondo problem, where the applied laser features the two circular polarizations with the same amplitude (i.e., a linear polarization) and thus couples equally to both spin states.

#### a. Single-channel spin-symmetric Rabi-Kondo

We start from the single-channel spin-symmetric Rabi-Kondo (1CSRK) problem. Now the Hamiltonian is

$$H_{1\text{CSRK}} = \frac{u}{4\pi} \int_{-\infty}^{\infty} dx [\partial_x \phi(x)]^2 + \frac{J_z}{\pi\sqrt{2}} P_K S_z \partial_x \phi(0) + \frac{J_{xy}}{2\pi a} P_K (S_+ e^{i\sqrt{2}\phi(0)} + \text{H.c.}) + 2\Omega \tau_x. \quad (\text{A12})$$

Here on the scale of  $T_K$  we obtain

$$H_{1\text{CSRK}}^{\text{int}} = \frac{u}{4\pi} \int_{-\infty}^{\infty} dx [\partial_x \phi(x)]^2 + \frac{J_{xy}^{\text{ren}}}{\pi a} P_K S_x + \Omega \tau_+ [P_{\uparrow} e^{-i\phi(0)/\sqrt{2}} + P_{\downarrow} e^{i\phi(0)/\sqrt{2}}] + \text{H.c.}, \quad (\text{A13})$$

which is invariant under flipping of  $S_z$ , together with the lead (integrated) spin density  $\phi(x)$ . However, this symmetry is not essential in the 1CK case, and the analysis goes basically the same as in the spin-asymmetric case (at least as long as one considers the spin-symmetric emission spectrum).

Let us note that one could formally map the secondary screening problem to an anisotropic spin-1 Kondo problem. Indeed, since  $J_{xy}^{\text{ren}}/(\pi a) \sim T_K$  is large, we can discard the  $S_x = -1/2$  state in the basis of Eq. (A13), and be left with three states: the Kondo state ( $\tau_z = 1$  and  $S_x = -1/2$ ) and the two spin states of the exciton ( $\tau_z = -1$  and arbitrary spin). Introducing corresponding spin-1 operators, the Hamiltonian would look like the single-channel spin-1 Kondo problem, after the non-spin-flip term has been eliminated by a transformation like those above, that modifies the exponents of the spin-flip term. However, this implies that the secondary  $J_z/(\pi u)$  is of order 1, i.e., the spin-1 problem is strongly spin anisotropic. Now, any spin exchange anisotropy would cause the creation of impurity-spin terms proportional to the square of the  $z$  component of the effective spin 1, which amounts to detuning the exciton and primary-Kondo states. For weak anisotropy, it is sufficient to add a corresponding compensating term to restore the degeneracy and hence the spin-1 Kondo physics. However, in our case, where the bare secondary exchange anisotropy is very large, the physics never reaches the underscreened spin-1 Kondo regime. Thus, the impurity entropy goes from  $\ln 4$  to  $\ln 3$  and then to zero as  $T$  is lowered through  $T_K$  and  $\Omega^*$ .

### b. Two-channel spin-symmetric Rabi-Kondo

The last case is the two-channel symmetric Rabi-Kondo (2CSRK) model, with Hamiltonian

$$H_{2CSRK} = \sum_{\ell=1,2} \left\{ \frac{u}{4\pi} \int_{-\infty}^{\infty} dx [\partial_x \phi_{\ell}(x)]^2 + \frac{J_z}{\pi\sqrt{2}} P_K S_z \partial_x \phi_{\ell}(0) + \frac{J_{xy}}{2\pi a} P_K (S_+ e^{i\sqrt{2}\phi_{\ell}(0)} + \text{H.c.}) \right\} + 2\Omega\tau_x, \quad (\text{A14})$$

which becomes on the scale of  $T_K$ :

$$H_{2CSRK}^{\text{int}} = \sum_{p=\pm} \frac{u}{4\pi} \int_{-\infty}^{\infty} dx [\partial_x \phi_{\ell}(x)]^2 + \frac{J_{xy}^{\text{ren}}}{\pi a} P_K S_x \cos[\phi_{-}(0)] + \Omega\tau_+ [P_{\uparrow} e^{-i\phi_+(0)/2} + P_{\downarrow} e^{+i\phi_+(0)/2}] + \text{H.c.} \quad (\text{A15})$$

Again the analysis parallels the spin-asymmetric case, except that now flipping  $S_z$  together with  $\phi_+(x)$  remains a symmetry, so the 2CK physics is not destroyed at low energies and a decoupled Majorana zero mode remains. Indeed, while the Rabi term contains  $S_z \propto S_x S_y$ , the corresponding processes are suppressed by the dominant  $J_{xy}^{\text{ren}}$  term, and all higher order processes (in terms of  $\Omega$ ) which leave the system within the low-energy manifold of  $J_{xy}^{\text{ren}}$  term do not couple to  $S_y$ . It should show up in the correlation function of the Rabi term with itself, which depends on  $S_z \propto S_x S_y$ , and reduce one power of  $\omega$  from the power-law dependence of the emission spectrum on  $\omega$  for  $|\omega| \ll T_K$ , that is, make it go as  $|\omega|^2$  instead of  $|\omega|^3$  (in the absence of detuning). Correspondingly, the impurity entropy goes from  $\ln 4$  to  $\ln(2 + \sqrt{2})$  to  $\ln \sqrt{2}$  as  $T$  is decreased through  $T_K$  and  $\Omega^*$ .

- 
- [1] C. Latta, F. Haupt, M. Hanl, A. Weichselbaum, M. Claassen, W. Wuester, P. Fallahi, S. Faelt, L. Glazman, J. von Delft, H. E. Türeci, and A. Imamoglu, *Nature* **474**, 627 (2011).
- [2] H. E. Türeci, M. Hanl, M. Claassen, A. Weichselbaum, T. Hecht, B. Braunecker, A. Govorov, L. Glazman, A. Imamoglu, and J. von Delft, *Phys. Rev. Lett.* **106**, 107402 (2011).
- [3] B. Sbierski, M. Hanl, A. Weichselbaum, H. E. Türeci, M. Goldstein, L. I. Glazman, J. von Delft, and A. Imamoglu, *Phys. Rev. Lett.* **111**, 157402 (2013).
- [4] P. Nozières and P. Blandin, *J. Phys.* **41**, 193 (1980).
- [5] A. M. Tsvelick and P. B. Wiegmann, *J. Stat. Phys.* **38**, 125 (1985).
- [6] A. M. Tsvelick, *J. Phys. C: Solid St. Phys.* **18**, 159 (1985).
- [7] N. Andrei and C. Destri, *Phys. Rev. Lett.* **52**, 364 (1984).
- [8] I. Affleck and A. W. W. Ludwig, *Phys. Rev. Lett.* **67**, 161 (1991).
- [9] I. Affleck and A. Ludwig, *Nucl. Phys. B* **360**, 641 (1991).
- [10] I. Affleck and A. W. W. Ludwig, *Phys. Rev. B* **48**, 7297 (1993).
- [11] V. J. Emery and S. Kivelson, *Phys. Rev. B* **46**, 10812 (1992).
- [12] V. J. Emery and S. A. Kivelson, *Phys. Rev. Lett.* **71**, 3701 (1993).
- [13] J. von Delft, G. Zaránd, and M. Fabrizio, *Phys. Rev. Lett.* **81**, 196 (1998).
- [14] G. Zaránd and J. von Delft, *Phys. Rev. B* **61**, 6918 (2000).
- [15] K. G. Wilson, *Rev. Mod. Phys.* **47**, 773 (1975).
- [16] R. Bulla, T. A. Costi, and T. Pruschke, *Rev. Mod. Phys.* **80**, 395 (2008).
- [17] A. Weichselbaum, *Phys. Rev. B* **86**, 245124 (2012).
- [18] A. Imamoglu, D. D. Awschalom, G. Burkard, D. P. DiVincenzo, D. Loss, M. Sherwin, and A. Small, *Phys. Rev. Lett.* **83**, 4204 (1999).
- [19] Y. Oreg and D. Goldhaber-Gordon, *Phys. Rev. Lett.* **90**, 136602 (2003).
- [20] A. A. Zvyagin and A. V. Makarova, *J. Phys.: Condens. Matter* **17**, 1251 (2005).
- [21] A. A. Zvyagin, V. Kataev, and B. Büchner, *Phys. Rev. B* **80**, 024412 (2009).
- [22] A. Weichselbaum, *Ann. Phys.* **327**, 2972 (2012).
- [23] P. Nozières, *J. Low Temp. Phys.* **17**, 31 (1974).
- [24] S.-S. B. Lee, J. Park, and H.-S. Sim, *Phys. Rev. Lett.* **114**, 057203 (2015).
- [25] I. Affleck and A. Ludwig, *J. Phys. A: Math. Gen.* **27**, 5375 (1994).
- [26] A. O. Gogolin, *Phys. Rev. Lett.* **71**, 2995 (1993).
- [27] N. V. Prokof'ev, *Phys. Rev. B* **49**, 2148 (1994).
- [28] P. W. Anderson and G. Yuval, *Phys. Rev. Lett.* **23**, 89 (1969).
- [29] G. Yuval and P. W. Anderson, *Phys. Rev. B* **1**, 1522 (1970).
- [30] P. W. Anderson, G. Yuval, and D. R. Hamann, *Phys. Rev. B* **1**, 4464 (1970).
- [31] P. B. Vigman and A. M. Finkel'Shtein, *Zh. Eksp. Teor. Fiz.* **75**, 204 (1978) [*Sov. Phys. JETP* **48**, 102 (1978)].
- [32] M. Fabrizio, A. O. Gogolin, and P. Nozières, *Phys. Rev. B* **51**, 16088 (1995).
- [33] M. Goldstein, Y. Weiss, and R. Berkovits, *EPL* **86**, 67012 (2009).
- [34] A. O. Gogolin, A. A. Nersesyan, and A. M. Tsvelik, *Bosonization and Strongly Correlated Systems* (Cambridge University Press, Cambridge, 2004).
- [35] J. Cardy, *Scaling and Renormalization in Statistical Physics* (Cambridge University Press, Cambridge, UK, 1996).
- [36] A. O. Gogolin and N. V. Prokof'ev, *Phys. Rev. B* **50**, 4921 (1994).
- [37] M. Fabrizio and A. O. Gogolin, *Phys. Rev. B* **50**, 17732(R) (1994).
- [38] M. Fabrizio and A. O. Gogolin, *Phys. Rev. B* **51**, 17827 (1995).
- [39] M. Goldstein and R. Berkovits, *Phys. Rev. B* **82**, 161307(R) (2010).